ELSEVIER

Polymer 41 (2000) 8879–8886

polymer

www.elsevier.nl/locate/polymer

On the multiple melting behavior of bisphenol-A polycarbonate

S. Sohn, A. Alizadeh, H. Marand*

Departments of Chemistry and Materials Science and Engineering, Virginia Polytechnic Institute and State University, Blacksburg, VA 24061-0212, USA

Received 7 September 1999; received in revised form 18 January 2000; accepted 19 January 2000

Abstract

Differential scanning calorimetry studies of the heating rate dependence of the multiple melting behavior of semicrystalline bisphenol A-polycarbonate (BAPC) are presented for different molar masses. In all cases, heating traces exhibit, in addition to the high temperature endothermic transition, a low endotherm located slightly above the crystallization temperature. After proper correction of the thermal lag effects, the high endotherm melting temperatures of the higher molar mass BAPC-19K and BAPC-28K samples are found to be independent of heating rate whether or not partial melting was carried out prior to recording the heating trace. These results demonstrate that the double melting behavior observed for high molar mass BAPC cannot be explained by a melting–recrystallization–remelting mechanism. In contrast, heating traces of the lower molar mass BAPC-4K sample exhibits two melting transitions within the high temperature endothermic region, which change both in magnitude and location with scanning rate, suggesting that melting–recrystallization–remelting can occur when chain mobility is sufficient to allow recrystallization. However, in all cases, the low and high endothermic regions are associated with the melting of two distinct populations of crystals, which have different thermal stability and are both present in the as-crystallized material. Crystallization studies after partial melting indicates that the low endotherm is associated with secondary crystals. The observed linear dependence of the melting temperature of secondary crystals with the square root of heating rate is consistent with superheating of secondary crystals. The origin of the superheating behavior is discussed in the context of conformational constraints in the residual amorphous fraction and the effect of crystallization time and molar mass on the low endotherm location.

Keywords: Multiple melting behavior; Endotherm; Secondary crystals

1. Introduction

Isothermally crystallized bisphenol A-polycarbonate (BAPC) [IUPAC name: poly(oxycarbonyloxy-1,4 phenylene isopropylidene-1,4phenylene)] exhibits a double melting behavior upon heating [1–3], similar to that displayed by many other polymers such as poly(ethylene terephthalate) (PET) [4], poly(butylene terephthalate) [5], poly(ether ether ketone) (PEEK)[6–9], poly(phenylene sulfide) [10], isotactic polystyrene [11–12], aliphatic polyamides [13], and ethylene/α-olefin copolymers [14]. The most common concepts invoked to explain the multiple melting behavior of semicrystalline polymers are: (1) melting of crystals of different stability [9–12,14]; and (2) a melting–recrystallization–remelting process [6,7,15]. It is fair to state that this apparently universal behavior is not completely understood.

In previous papers, we demonstrated that the concept of melting–recrystallization–remelting does not explain the multiple melting phenomenon observed for ethylene/1-octene copolymers [14] and PEEK [9]. We also noted that the low endotherm melting temperature, after correction for thermal lag effects, still exhibits a significant heating rate dependence in the case of PEEK. Since the effect of heating rate on the observed multiple melting behavior, is generally used as a justification for the existence of reorganization effects, it is worthwhile to address this issue more thoroughly. Specifically, it is imperative to examine whether such heating rate dependence is consistent with the explanation of the multiple melting behaviors in terms of a bimodal population of crystals of different morphological characteristics. In this paper, we use loosely the term reorganization during heating as implying melting–recrystallization–remelting, although we realize that reorganization can also occur through lamellar thickening or increase in crystal perfection.

We have also recently discussed the effect of topological constraints on the secondary crystallization of ethylene/1-octene random copolymers [14], PEEK [9,17], isotactic poly(styrene) (it-PS) [16,17] and PET [16,17]. A number of apparently universal features of the secondary crystallization process has emerged from these studies, even though the nature of the topological constraints may be different for different classes of polymers [16]. In the case

* Corresponding author. Tel.: 1-540-231-8227; fax: 1-540-231-8517.
E-mail address: hmarand@chemserver.chem.vt.edu (H. Marand).

0032-3861/00/$ - see front matter
PII: S0032-3861(00)00110-5

Table 1
Molecular characteristics and crystallization conditions of bisphenol-A polycarbonate samples

Sample	M_w (g mol^{-1})	M_w/M_n	Crystallization conditions	ΔH_m^{total} (J/g)
BAPC-4K	4300	1.02	165°C, 38 h	34.4
BAPC-19K	18800	1.99	170°C, 384 h	27.2
BAPC-28K	28400	2.07	185°C, 202 h	25.9

of ethylene/1-octene random copolymers, the constraints are structural in nature and are associated with the presence of hexyl branches along the polyethylene backbone. A given copolymer chain is characterized by a distribution of crystallizable sequence lengths. While some of the methylene sequences are long enough to participate in lamellar growth by a chain folding mechanism (primary crystallization), others are too short to form stable lamellae and can only crystallize through a clustering process and form fringed micellar structures (secondary crystallization). On the contrary, in the case of materials such as PEEK and PET, conformational constraints arise from the intrinsic local stiffness of the chains and their aversion toward adjacent reentry folding during primary crystallization. Secondary crystallization in these materials is also envisioned to occur through clustering of chain segments belonging to cilia, loose folds and tie chains in the interlamellar amorphous phase [12,16,17]. In all cases, the initial stage of secondary crystallization is characterized by an Avrami exponent of 1/2. The secondary crystallization process is then, from a mechanistic standpoint, significantly different from primary crystallization, which is usually described by a model of nucleation-controlled growth with Avrami exponent in the range of 2 to 4. Primary crystallization from the free unconstrained melt yields chain folded lamellar structures, while secondary crystallization takes place from a constrained amorphous phase and gives rise to fringed micellar structures at high undercoolings and mosaic-block crystals at lower undercoolings. Secondary crystallization has also been found to result in a shift to longer times or to higher temperatures of the relaxation spectrum associated with the glass to rubber transition [9,16,17] similar to that observed during the crosslinking of an amorphous polymer.

In the present paper, we investigate the multiple melting behavior of BAPC in some detail. The exceedingly slow crystallization of BAPC makes it an excellent candidate for this study, since the different stages of crystallization and melting can be easily separated. We examine the circumstances under which reorganization by melting and recrystallization can be observed during heating and conclude that, as in PEEK [9], such effects, when present, affect primarily the shape of the upper melting endotherm. We demonstrate that the multiple melting phenomenon universally observed after isothermal crystallization in semiflexible chain polymers is in general not explained by a mechanism of melting–recrystallization–remelting. In contrast, we find support for the proposal that the double endothermic phenomenon is associated with the melting of crystals, which differ in thermal stability and in morphological characteristics.

2. Experimental

2.1. Materials characterization

Two of the bisphenol-A polycarbonate samples investigated in this work are commercial grades from General Electric under the trade name Lexan™. These samples are denoted BAPC-19K and BAPC-28K to indicate differences in their weight average molar masses. We also briefly discuss the study of a narrow molar mass sample (BAPC-4K) obtained by solution fractionation of the commercial BAPC-28K sample. The experimental details for the fractionation procedure are described in a companion paper [18] dealing with secondary crystallization of BAPC fractions and bulk material. The commercial samples were purified by sequential dissolution in chloroform, filtration and precipitation in methanol. These samples were washed several times with clean methanol and then dried under vacuum at 150°C for a period of 24 h to remove possible traces of solvent. Their weight average molar mass and polydispersity index, obtained by gel permeation chromatography in $CHCl_3$ at room temperature, are listed in Table 1. In order to avoid degradation of BAPC during residence at high temperature, the samples were further dried for 24 h under vacuum above their glass transition temperature and kept in a dessicator prior to crystallization. Amorphous films, 120 ± 20 μm thick, were prepared under a nitrogen atmosphere by compression molding of the dried samples at 250°C for 5 min under a pressure of 150 psi, and subsequent cooling to room temperature. The amorphous films thus prepared were then isothermally crystallized from the glassy state under an inert atmosphere. Under the crystallization conditions employed here these samples nearly achieve their maximum heat of fusion (see Table 1). Analysis of the crystallized BAPC samples by GPC confirm that residence at the high crystallization temperature for extended periods of time did not adversely affect their molar mass distribution.

2.2. Differential scanning calorimetry

The thermal behavior of these samples was investigated by differential scanning calorimetry using Perkin–Elmer DSC-2 operated under nitrogen purge with an ice/water heat sink. In order to reduce differences among samples due to thermal lag, similar discoid samples of 120 ± 20 μm thickness and 11.0 ± 1.0 mg mass were employed. Both heating and cooling experiments were performed at different scanning rates ranging from 0.3 to 40°C/min. The heat capacity calibration was carried out using a sapphire standard after empty pan subtraction. The temperature calibration during the cooling scans was achieved by

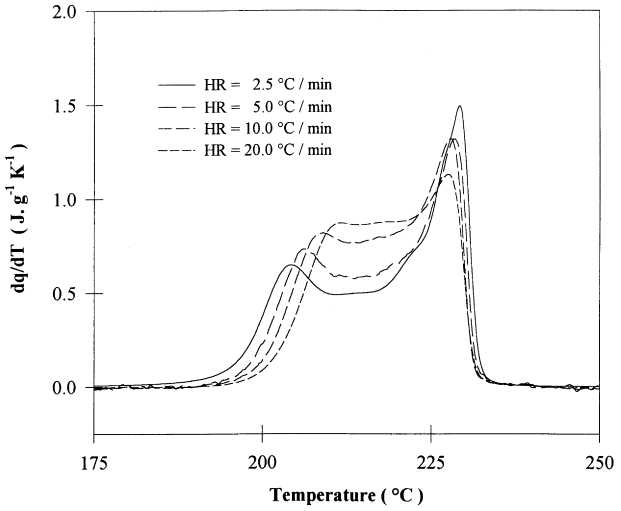

Fig. 1. Effect of heating rate on the melting behavior of BAPC-28K crystallized at 185°C from the glassy state for 202 h and quenched to 100°C.

recording the isotropic-to-nematic phase transition of azoxyanisole ($T_{I/N} = 136.0$°C). The temperature calibration during heating scans was accomplished by recording the melting transition of an indium standard sandwiched between two amorphous BAPC films. Finally, crystallization temperatures during isothermal treatments were calibrated by extrapolating the melting temperatures of standards (tin, lead and indium) to zero heating rate. In all cases, DSC traces are presented after subtraction of a baseline, which approximates the heat capacity of the semicrystalline sample over the temperature range considered. Use of a linear baseline in the melting region was mandated by the lack of availability of heat capacity data for the crystal phase of bisphenol-A polycarbonate. Therefore, the heating traces presented in this paper only provide information on enthalpic contributions associated with the melting process. Consequently, apparent heat capacities (dq/dT) will vanish above and below the melting transition.

3. Results and discussion

3.1. Nature of the multiple melting behavior in BAPC

A multiple melting behavior arising from melting–recrystallization–remelting during heating generally exhibits a strong heating rate dependence [15,19]. At low heating rates, there is sufficient time for melting of initially present crystals and recrystallization during the heating scan. In this case, the low endotherm is a net result of the superposition of the melting endotherm of initial crystals and the recrystallization exotherm of the just molten material. The high endotherm is then observed at temperatures where recrystallization effects are no longer significant and where the melting of crystals formed during the heating scan becomes dominant. At high heating rates, initially present crystals melt during the heating scan but recrystallization cannot take place since the residence time at temperatures where crystallization could take place becomes too short. In this case, a single melting endotherm is observed. Therefore in the case of melting–recrystallization–remelting processes during heating, an increase in heating rate should lead to a shift of the high endotherm to lower temperatures and a decrease in the relative magnitude of the high endotherm viz., that of the low endotherm. To avoid such processes during heating, one should carry out the DSC experiment at high heating rates. Unfortunately under these conditions, thermal lag effects lead to a broadening and a shift to higher temperatures of the observed endothermic transition [19]. Commonly, metal standards are used to calibrate the temperature scale at a given heating rate. However, since the thermal conductivity of organic materials is much lower than that of metals, use of pure metal standards leads to an inadequate temperature calibration and, more importantly, does not allow to correct the shape of the melting endotherm for the effect of temperature gradients within the sample. We therefore carried out the temperature calibration using an indium standard sandwiched between two amorphous BAPC films and subsequently used Gray's method [20,21] to correct for the effect of heating rate on the endotherm shape.

Table 2
Melting temperatures of BAPC-28 after and before partial melting

Heating rate (°C/min)	BAPC-28K (original) crystallized at 185°C for 202 h		PM;BAPC-28K Partially melted at 220°C
	T_m^{low} (°C)	T_m^{high} (°C)	T_m^{high} (°C)
2.5	204.0	229.1	228.9
5.0	205.6	228.5	228.2
10.0	207.2	227.8	228.6
20.0	208.9	228.4	228.7

In Fig. 1, the corrected heating traces of BAPC-28K crystallized for 202 h at 185°C by heating from the glassy state are displayed for heating rates, β, ranging from 2.5 to 20°C/min. Heating of BAPC-28K subsequent to the above crystallization process gives rise to a low, an intermediate and a high melting endotherm. The intermediate endotherm spreads over a wide temperature range and under this particular crystallization condition overlaps with both low and high melting endotherms. As can be observed in Fig. 1 and in Table 2, the location of the high endotherm is found to be independent of heating rate (for $\beta > 2$°C/min). On the contrary, the low endotherm shifts systematically towards higher temperatures with increasing heating rate. The total heat of fusion of the sample (25.9 J/g) is independent of heating rate.

We now focus on the results of similar experiments carried out for BAPC-4K. In Fig. 2, we show DSC heating traces obtained after crystallization at 165°C for 38 h at scanning rates ranging from 5 to 20°C/min. In each case three endotherms are detected. The lower endotherm is

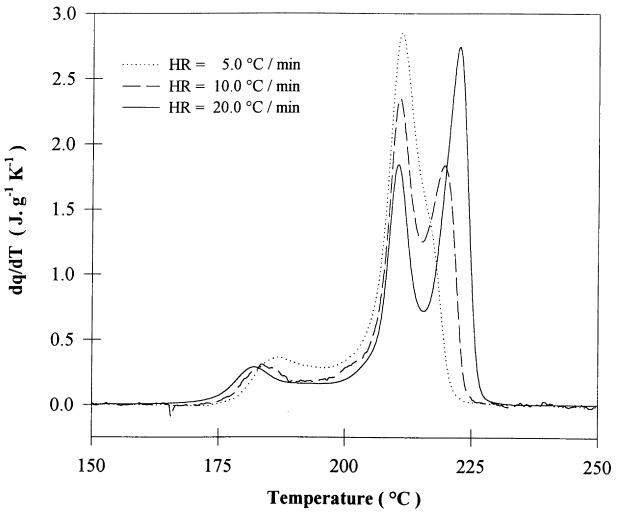

Fig. 2. Effect of heating rate on the melting behavior of BAPC-4K crystallized at 165°C from the glassy state for 38 h and quenched to 100°C.

observed slightly above the crystallization temperature and shifts to higher temperatures with increasing heating rate. The upper endothermic region shows the trend expected for a melting–recrystallization–remelting phenomenon. The enthalpy of fusion of the intermediate endotherm increases and that of the highest endotherm decreases with increasing heating rate. Further, the intermediate endotherm shifts to higher temperatures while the highest endotherm shifts to lower temperatures with increasing heating rate. A similar increase in the rate of reorganization during heating with decreasing molar mass has been reported for poly(vinylidene fluoride), nylon-12 and poly(phenylene sulfide) by Judovits et al. [22].

Partial melting experiments were carried out by heating ($\beta = 20$°C/min) BAPC-28K samples crystallized at 185°C for 202 h slightly above the peak temperature of the low endotherm, (i.e. 220°C). Upon reaching 220°C, these samples were cooled to 100°C at a rate of −40°C/min and subsequently reheated at various rates to record their melting behavior. The corrected heating traces of partially melted BAPC-28K (PM;BAPC-28K) samples are shown in Fig. 3 for rates ranging from 2.5 to 20°C/min. PM;BAPC-28K samples solely exhibit a high endotherm whose corresponding peak melting temperature (see Table 2) and heat of fusion are found to be heating rate independent. The average heat of fusion of the partially melted samples is equal to 8.4 J/g. The high endotherm melting temperature, T_m^{high}, of the original sample (third column) is found to be identical, within experimental error, to that of the partially melted sample (fourth column) for all heating rates.

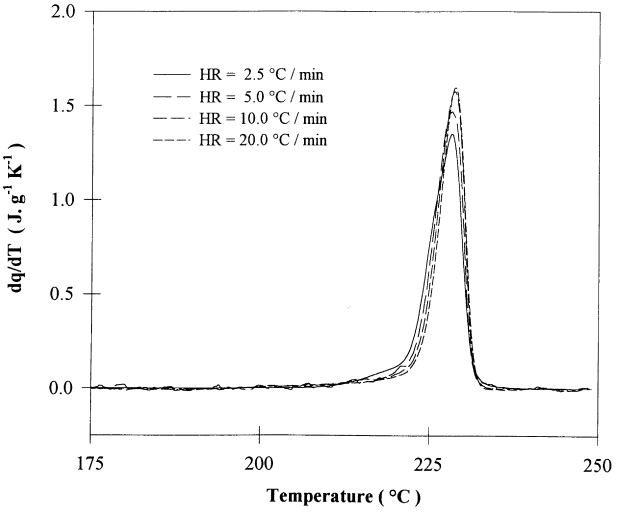

Fig. 3. Effect of heating rate on the melting behavior of BAPC-28K crystallized at 185°C from the glassy state for 202 h, partially melted at 220°C and quenched to 100°C.

The observations, for higher molar mass BAPC materials, that partially melted samples exhibit exclusively the higher endothermic transition and that identical peak temperatures are obtained for the high endotherm in the original and partially melted samples lead us to conclude that the multiple melting behavior is associated with the fusion of crystals exhibiting different morphologies and stabilities. For high molar mass BAPC samples, the high endotherm does not arise from reorganization processes taking place during heating but is associated with the melting of primary (lamellar) crystals. For both high and low molar mass samples, the low endotherm is associated with the melting of crystals formed during secondary crystallization.

In the previous set of experiments, we investigated separately the characteristics of the high and low endotherms by direct comparison of heating traces of as-crystallized and partially melted BAPC samples. This comparison is based on the assumption that partial melting and subsequent cooling of the samples do not affect the population and the size of the most stable primary crystals. The observation of identical peak melting temperatures for as-crystallized and partially melted samples indicates that the heating rate and the upper temperature used for partial melting were properly chosen to avoid reorganization of the primary crystals. In order to investigate the melting characteristics of secondary crystals, it is important to ensure that there is no morphological evolution during cooling between the upper temperature used for partial melting and the temperature at which secondary crystallization is performed (see below). We therefore need to discuss the influence of the rate of cooling from 220 to 100°C on the subsequent melting behavior. Fig. 4 shows the melting traces of a series of PM;BAPC-28K samples, which were cooled to 100°C at different rates ranging from $\beta = -0.3$ to −40°C/min. The heating traces were recorded at a constant rate of 10°C/min. We note that the melting trace of a partially melted sample is independent of cooling rate for rates in excess of 2.5°C/min. However, for cooling rates lower or equal to 2.5°C/min, both the enthalpy of fusion and the peak melting temperature increase with decreasing cooling rate. A close inspection

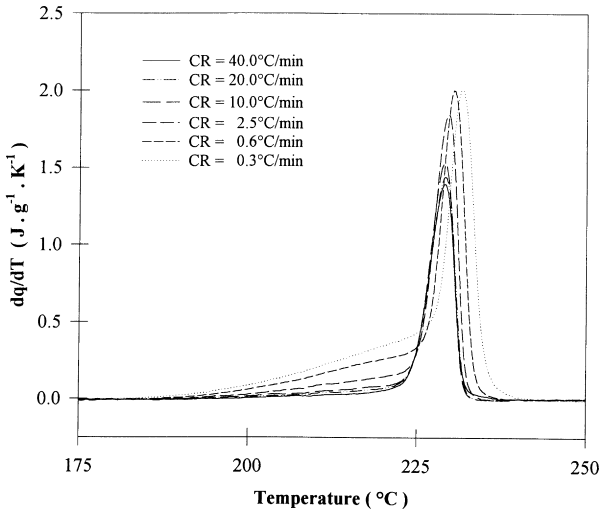

Fig. 4. Effect of cooling rate on the melting behavior of BAPC-28K crystallized at 185°C from the glassy state for 202 h, partially melted at 220°C and cooled to room temperature.

of Fig. 4 also reveals that the melting process of rapidly cooled PM;BAPC-28K samples ($|\beta| \geq 10$°C/min) occurs in a relatively narrow temperature range. In contrast, the onset of melting in samples cooled more slowly between 220 and 100°C is observed at much lower temperatures. These observations indicate that during slow cooling ($|\beta| \leq$ 2.5°C/min) further crystallization can take place in the partially melted samples. Note that upon cooling an initially amorphous BAPC from the melt, even at scanning rates much lower than those used here, no perceptible crystallization occurs. This is due to the large induction time associated with the crystallization of BAPC from the free melt [23–25]. However, in presence of already existing crystals, (i.e. those left after partial melting), and possibly because of conformational constraints present in the residual amorphous fraction, the crystallization rate is noticeably enhanced. This phenomenon has been previously reported in the literature [3–18] and is discussed below in more detail. The shift of the melting endotherm to higher temperatures with decreasing cooling rate (see Fig. 4) suggests either that lamellar thickening may be operative in BAPC crystals at temperatures in the vicinity of 200–220°C or that some crystals form during cooling between 220 and 185°C. These crystals would indeed be expected to be more stable than those formed during the initial crystallization at 185°C. However, in this case the heating trace might be expected to exhibit multiple peaks or at least a high temperature shoulder. The observation of a single, relatively narrow endotherm suggests that both processes (lamellar thickening and new crystal formation) may be at play. The occurrence of lamellar thickening by annealing at temperatures above 208°C has actually been evidenced through atomic force microscopy and will be the subject of a subsequent paper [26]. In conclusion, longer residence at temperatures in the range 220–185°C during cooling leads to an increase in crystallinity. We emphasize, however, that such effects are only observed for extremely low cooling rates.

The occurrence of reorganization processes (melting–recrystallization–remelting and/or lamellar thickening) in the high endotherm region is therefore a function of the sample molar mass, and the scanning rate during heating or cooling in the case of partially melted samples. We mentioned earlier that the induction period for the crystallization of BAPC chain segments is much shorter when crystals are already present than when crystallization occurs from the free melt. Studies of the effect of cooling rate after partial melting indicate that further crystallization can indeed occur if sufficient time is given for this process (cooling rates less than 2.5°C/min). This suggests that the rate of formation of new crystals is enhanced either when other crystals are already present or if previous melting has not led to a totally relaxed amorphous fraction. Under both circumstances, the energy barrier for crystal nucleation appears to be reduced. In a separate study of secondary crystallization of BAPC we show that the induction periods for the primary and secondary crystallization of BAPC-28K at 185°C differ by three orders of magnitude (48 h and 1 min, respectively) [18]. This clearly suggests a difference in mechanism between primary and secondary crystallization. During partial melting, chain segments in secondary crystals loose crystallographic registration but cannot return to the random conformational state characteristic of the unconstrained molten phase. This is likely to be a consequence of both the rigid backbone structure of BAPC and the constraints exerted by surrounding primary crystals.

We also noted that for both BAPC [18] and PEEK [9], the low endotherm position is identical for as-crystallized samples and for samples that were partially melted and further crystallized at the initial temperature. Since the melting temperature of secondary crystals formed at a given temperature has been suggested to reflect, at least in part, the conformational entropy of the surrounding liquid [9,16,17], it follows that partial melting leads to the same local melt entropy as characteristic of the amorphous phase prior to secondary crystallization. In other words, chain segments which participate in the secondary crystallization process at some temperature T exhibit the same conformational entropy after partial melting and quench to T as they did at the beginning of secondary crystallization at T without partial melting. A lower conformational entropy of the residual amorphous fraction may be at the origin of both the much shorter induction time for secondary crystallization, and the fact the resulting secondary crystals can exhibit superheating effects (see later).

In summary, the results presented in this section allow us to establish the specific conditions necessary to avoid further crystallization during cooling of partially melted samples and also to prevent reorganization during heating. Further, we will show in a separate publication that for high molar mass BAPC samples the high endotherm location and

Table 3
Heating rate parameters for secondary crystallization under different conditions. (PM: partial melting at 220°C; SC for secondary crystallization at the indicated temperature; β: heating rate in °C/min)

Samples	Crystallization conditions	$T_m^{low} = (T_m^{low})^\circ + K\beta^{1/2}$	
		$(T_m^{low})^\circ$	K
BAPC-28K	185°C, 202 h	202.2	1.52
PM; BAPC-28K	SC:175°C, 120 min	189.7	1.50
	SC: 185°C, 40 min	196.7	1.49
	SC: 185°C, 120 min	199.2	1.56
BAPC-19K	170°C, 384 h	189.9	1.50
PM; BAPC-19K	SC: 170°C, 120 min	181.5	1.49
BAPC-4K	165°C, 38 h	176.5	2.18

heat of fusion associated with primary crystals formed at 185°C are not affected by isothermal treatments as long as 200 min in the range 165–185°C and 10 min in the range 195–223°C [26].

3.2. Heating rate dependence of the low endotherm

Secondary crystallization experiments were conducted at different temperatures with a series of partially melted BAPC samples. After partial melting at 220°C, the samples were immediately quenched to a temperature T_x, where further crystallization was allowed for a given time T_x (see Table 3). Note that in all cases the temperature, T_x, associated with this crystallization stage is below or equal to the primary crystallization temperature. According to the results presented in the previous section, we do not expect the morphological characteristics exhibited by primary crystals to be affected by the secondary crystallization process.

In Fig. 5 the heating traces of partially melted BAPC-28K before and after secondary crystallization at 185°C for

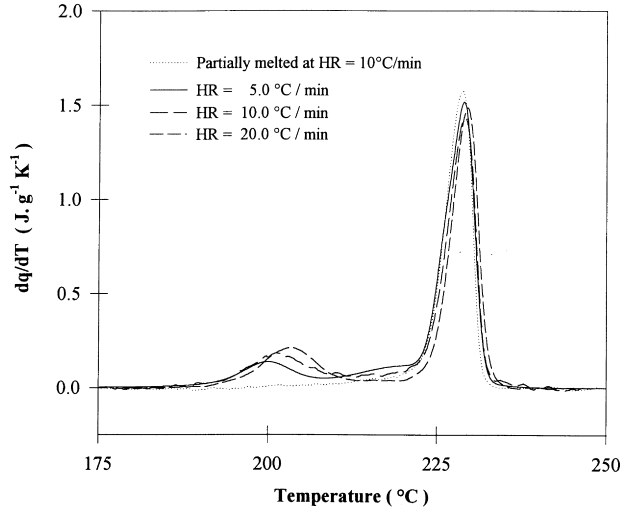

Fig. 5. Effect of heating rate on the melting behavior of BAPC-28K crystallized at 185°C from the glassy state for 202 h, partially melted at 220°C and recrystallized at 185°C for 40 min.

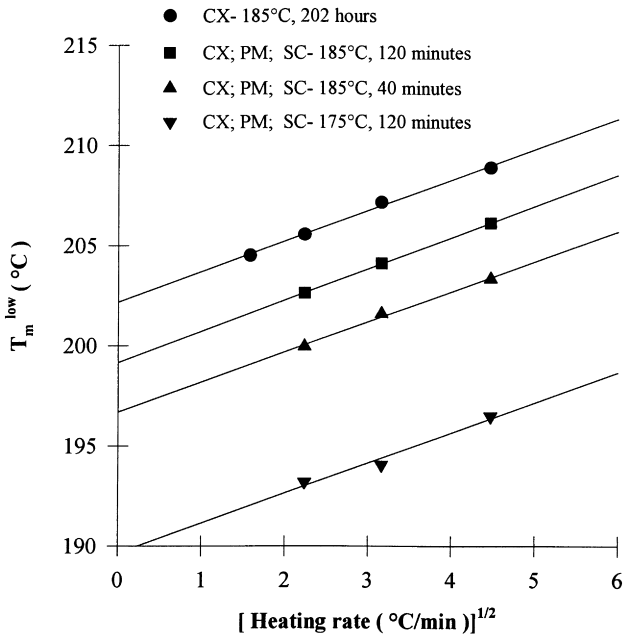

Fig. 6. Effect of heating rate on the low endotherm location of BAPC-28K crystallized under various conditions.

40 min are displayed for heating rates in the range 5–20°C/min. Comparing the 10°C/min heating trace of the partially melted samples with and without further crystallization at 185°C confirms once more that both the location and the heat of fusion of the high endotherm are not affected by the second thermal treatment at 185°C. Crystallization at 185°C after partial melting leads to the development of a low endotherm observed just above the crystallization temperature. Further, the low endotherm melting temperature increases steadily with heating rate. Similar results are observed for crystallization at different temperatures after partial melting. On closer examination of Fig. 5 we also note that at the lowest heating rate (5°C/min), a small shoulder develops between the low and high endotherms. The overall enthalpy of fusion associated with the low endotherm and shoulder appears to remain independent of heating rate. This observation suggests that secondary crystals may undergo a small extent of reorganization by melting–recrystallization–remelting during slow heating. However, we emphasize that the extent of reorganization, as indicated by the enthalpy of fusion associated with the shoulder, is small and will not affect significantly the location of the low endotherm peak melting temperature. We also emphasize that reorganization processes in the low endothermic region are not present for heating rates exceeding 10°C/min. These latter observations provide additional and strong support for our claim that the low and high endotherms are associated with the melting of two different morphological entities. These results also suggest that temperature modulated DSC may not be the most appropriate tool to investigate the melting behavior of as-formed secondary crystals since this technique relies on the use of very low heating

rates, at which reorganization processes can become significant.

In Fig. 6, the low endotherm melting temperature, T_m^{low}, is plotted as a function of the square root of heating rate, $\beta^{1/2}$, for different secondary crystallization conditions. The use of this particular graphic representation is discussed later. In Fig. 6 we have also included the data corresponding to the original sample crystallized at 185°C for 202 h. In all cases, and in line with previous results obtained with PEEK, isotactic polystyrene and PET [17], T_m^{low} is well described by a linear function of $\beta^{1/2}$. Moreover, the slopes of the various T_m^{low} vs $\beta^{1/2}$ line are identical within experimental error (see Table 3, BAPC-28K exhibits an average slope of 1.52 ± 0.03). It is important to recognize that a constant value for the slopes of T_m^{low} vs $\beta^{1/2}$ lines is incompatible with the account of the multiple melting behavior by a melting–recrystallization–remelting process. We do acknowledge that the upward shift of the low endotherm with increasing heating rate is itself compatible with the occurrence of melting–recrystallization–remelting during heating. We note, however, that the same dependence of melting temperature on heating rate is displayed for crystals exhibiting intrinsically different thermal stabilities. For instance, the same slope of $T_m^{low} - \beta^{1/2}$ is observed for crystals formed at 185°C over a period of 202 h, (more stable) and for crystals formed at 175°C for 120 min (less stable). Such behavior is incompatible with expectations for melting–recrystallization–remelting phenomena.

A clue for the origin of the heating rate dependence of the low endotherm melting temperature is obtained from the linearity of T_m^{low} vs $\beta^{1/2}$ plots after thermal lag correction. This observed behavior has been shown by Strobl and coworkers to be a characteristic of superheated crystals [27]. Superheating is a term used to describe the melting of a crystal at a temperature above that expected from equilibrium considerations. To obtain the linear dependence between T_m^{low} and $\beta^{1/2}$, the rate of melting must be assumed to be a linear function of the degree of superheating [19,27]. Using temperature modulated differential scanning calorimetry Toda et al. [28] recently showed that the hypothesis of a linear dependence of the rate of melting on superheating may be oversimplified. According to Toda et al. [28] a rate of melting proportional to ΔT^y, leads to a linear variation of the degree of superheating with $\beta^{1/(1+y)}$. At this point it is not possible for us to accurately determine the value of y. However, a value of y in the vicinity of 0.5 yields an acceptable fit of our experimental data.

The degree of superheating of a specific crystal at a given heating rate, β, is defined as the difference between the melting temperature at that heating rate, in our case, T_m^{low}, and the equilibrium or zero entropy production melting temperature of that crystal, $(T_m^{low})^\circ$. In polymeric materials, two types of crystal morphologies lend themselves to superheating [19]. First, in materials such as polyethylene or polytetrafluoroethylene extended chain crystals, superheating is due to the slow kinetics of melting large crystals. Second, metastable crystals with conformationally constrained interfacial chains such as tie chains or loose loops will also exhibit reduced entropy of fusion upon melting (i.e. show superheating). The increase in the melting temperature of secondary crystals with heating rate, observed in our study, is most likely associated with the latter case. Such reduction in entropy of fusion has already been discussed by Wunderlich [19] and Zachmann [29] in the context of fringed micellar structures. As mentioned earlier, previous investigations strongly suggest that the low endotherm in many semicrystalline polymers is associated with the melting of bundle-like or fringed micellar secondary crystals [9,14,16]. The formation of fringed micellar structures during secondary crystallization has a profound influence on the remaining amorphous phase. Secondary crystallization leads to an increase in the level of conformational constraints, thus to a reduction in the conformation entropy of the remaining amorphous phase. In support of this point of view, both the glass transition and the low endotherm melting temperatures are found to shift to higher temperatures with increasing secondary crystallization time. Theoretical support for this idea has been recently obtained from thermodynamic correlations between the temporal evolution of the melting temperature of secondary crystals and that of the glass transition temperature of the residual amorphous fraction [17]. This thermodynamic model was successfully applied to experimental data on it-PS, PEEK and PET. All the above arguments suggests that the shift of the low endotherm to higher temperature with increasing heating rate, is compatible with superheating of metastable fringed micellar crystals.

As a final argument supporting the applicability of superheating concepts in the case of secondary crystals, we compare the degree of superheating, $T_m^{low} - (T_m^{low})^\circ$, for BAPC samples of varying molar masses. Examination of Table 3 indicates that the slope K, which is directly related to the degree of superheating, is considerably larger for BAPC-4K than for the other two BAPC samples. In a parallel study, we also found that rate of shift of the low endotherm with secondary crystallization time is significantly larger for BAPC-4K than for BAPC-19K and BAPC-28K [18]. Studies of narrow molar mass fractions indicate that this difference in behavior is not associated with the broader molar mass distribution of BAPC-19K and BAPC-28K. The increase in both the superheating effects and the rate of shift of the low endotherm melting temperature with secondary crystallization time for lower molar mass materials is most likely explained by the increase in primary crystallinity and the resulting rise in conformational constraints in the residual amorphous fraction with decreasing molar mass. In support for this interpretation, we note that studies of poly(phenylene sulfide) by Cebe et al. [30] indicate that the content in rigid amorphous fraction increases with decreasing molar mass.

4. Conclusions

Studies of the heating rate dependence of the melting behavior of semicrystalline bisphenol-A polycarbonate of various molar masses indicate that the high and low endothermic regions are associated with the melting of primary and secondary crystals, respectively. No reorganization effects during heating are observed for BAPC-19K and BAPC-28K in the usual range of scanning rates ($\beta >$ 2.5°C/min). In contrast, the lower molar mass material, BAPC-4K, exhibits a melting–recrystallization–remelting process during heating. However, this reorganization process, which is mediated by the higher mobility, thus higher recrystallization rate of the shorter chain length polymer, only affects the shape of the high endothermic region. The observed upward shift of the low endotherm with increasing heating rate is explained by superheating effects and is fully consistent with the notion that amorphous chains in the vicinity of secondary crystals are conformationally constrained and that these constraints do not fully relax upon melting the secondary crystals.

Acknowledgements

We gratefully acknowledge funding of this work by the National Science Foundation Science and Technology Center for High Performance Polymeric Adhesives and Composites at Virginia Tech (DMR-91-20004) and by a National Science Foundation Young Investigator Award (DMR-93-57512). We also thank L. Schank and H.D. Iler for supplying the BAPC-4K fraction.

References

[1] Beckman E, Porter RS. J Polym Sci, Polym Phys Ed 1987;25:1511.
[2] Laredo E, Grimau M, Müller A, Bello A, Suarez N. J Polym Sci, Polym Phys Ed 1996;34:2863.
[3] Mendez G, Müller AJ. J Thermal Anal 1997;50:593.
[4] Roberts RC. J Polym Sci B 1970;8:381.
[5] Yeh JT, Runt J. J Polym Sci, Polym Phys Ed 1989;27:1543.
[6] Blundell DJ, Osborn BN. Polymer 1983;24:953.
[7] Lee Y, Porter RS. Macromolecules 1989;22:1756.
[8] Marand H, Prasad A. Macromolecules 1992;25:1731.
[9] Marand H, Alizadeh A, Farmer R, Desai R, Velikov V. Macromolecules 2000;33 (in press).
[10] Chung JS, Cebe P. Polymer 1992;33(11):2312.
[11] Lemstra PJ, Koistra T, Challa G. J Polym Sci A-2 1972;10:823.
[12] Lemstra PJ, Schouten AJ, Challa G. J Polym Sci, Polym Phys Ed 1974;12:1565.
[13] Bell JP, Dumbleton JH. J Polym Sci A-2 1969;7:1033.
[14] Alizadeh A, Richardson L, Xu J, Marand H, Cheung W, Chum S. Macromolecules 1999;32:6221.
[15] Rim PB, Runt JP. Macromolecules 1984;17:1520.
[16] Marand H, Alizadeh A, Farmer R, Elkoun S. In preparation.
[17] Marand H, Alizadeh A. In preparation.
[18] Alizadeh A, Sohn S, Marand H, Schank L, Iler HD. In preparation.
[19] Wunderlich B. Macromolecular physics, vol 3. New York: Academic Press, 1976.
[20] Gray A. Analytical chemistry, vol 1. New York: Plenum Press, 1963. p. 322.
[21] Berstein V, Ergov VM. Differential scanning calorimetry of polymers. Physics, chemistry, analysis, technology. Chichester, UK: Ellis Horwood, 1994.
[22] Judovits L, Menczel JD, Leray A-G. J Thermal Anal 1998;54:605.
[23] MacNulty BJ. Polymer 1968;9:41.
[24] Kampf G. Kolloid-Z 1960;172:50.
[25] Siegmann A, Geil PH. J Macromol Sci, Phys 1970;B4(2):273.
[26] Sohn S, Marand H. In preparation.
[27] Schawe JEK, Strobl GR. Polymer 1998;39:3745.
[28] Toda A, Oda T, Tomita C, Hikosaka M, Arita T, Saruyama Y. Proc Am Chem Soc, Polym Div 1999;81:236.
[29] Zachmann HG, Peterlin A. J Macromol Sci, Phys 1969;B3(3):495.
[30] Lu SX, Cebe P, Capel M. Macromolecules 1997;30(20):6243.